https://doi.org/10.2352/ISSN.2470-1173.2021.17.AVM-186

Contrast Signal to Noise Ratio

Robin Jenkin, NVIDIA Corporation

Abstract

The detection and recognition of objects is essential for the operation of autonomous vehicles and robots. Designing and predicting the performance of camera systems intended to supply information to neural networks and vision algorithms is non-trivial. Optimization has to occur across many parameters, such as focal length, f-number, pixel and sensor size, exposure regime and transmission schemes. As such numerous metrics are being explored to assist with these design choices. Detectability index (SNR_I) is derived from signal detection theory as applied to imaging systems and is used to estimate the ability of a system to statistically distinguish objects [1], most notably in the medical imaging and defense fields [2].

A new metric is proposed, Contrast Signal to Noise Ratio (CSNR), which is calculated simply as mean contrast divided by the standard deviation of the contrast. This is distinct from contrast to noise ratio which uses the noise of the image as the denominator [3,4]. It is shown mathematically that the metric is proportional to the idealized observer for a cobblestone target and a constant may be calculated to estimate SNR_I from CSNR, accounting for target size. Results are further compared to Contrast Detection Probability (CDP), which is a relatively new objective image quality metric proposed within IEEE P2020 to rank the performance of camera systems intended for use in autonomous vehicles [5]. CSNR is shown to generate information in illumination and contrast conditions where CDP saturates and further can be modified to provide CDP-like results.

Introduction

The design of camera systems is crucial to yielding good detection performance for autonomous driving systems. To facilitate this, objective metrics are needed that correlate to the overall performance of the system and the challenge of creating them is non-trivial. Metrics need to work for a wide variety of illumination conditions and to account for a large number of system parameters. Ideally metrics should also be predictive as to avoid unnecessary construction of hardware. The IEEE P2020 Image Quality for Autonomous Vehicles standard group has undertaken the task to adapt existing and develop new metrics for such purposes [6].

Contrast detection probability (CDP) is an empirical metric proposed by Geese et al. [5] as an IEEE P2020 metric to predict computer vision performance for autonomous vehicles. It is based on the premise that it is the ability of an imaging system to record contrast between a target and background and its interaction with noise that predominantly determines the ability to detect objects. By examining a distribution of contrasts, CDP estimates the spread of contrast due to noise in the system and calculates the probability that measured contrasts will fall within given bounds [5]. It is suggested by Geese et al. that the bounds may be set according to the application and desired level of visibility [5].

This paper introduces another metric, contrast signal to noise ratio (CSNR) which may be calculated using the same data as CDP. It is demonstrated CSNR may be calculated without prior choice of thresholds and that system performance may be derived in areas where CDP saturates. CSNR is also shown mathematically to be proportional to the idealized observer calculated for a cobblestone target.

Contrast Detection Probability

Geese *et al.* define CDP as [5]:

$$CDP_{K_{IN}} = P\left(K_{IN}(1-\varepsilon) \le K_M \le K_{IN}(1+\varepsilon)\right) \quad (1)$$

where, K_{IN}, is input contrast, K_M, measured contrast, ε, contrast bounds and $P()$ probability. CDP is the probability that the contrast calculated from two randomly selected pixels will fall between given bounds. Weber, Michelson, or a simple difference may be used to calculate contrast [5]. In this work we use Weber contrast, K_W, to perform the calculation, defined below:

$$K_W = \frac{E_{MAX}}{E_{MIN}} - 1 \quad (2)$$

where E_{MAX} and E_{MIN} represent the maximum and minimum signal respectively.

Practical calculation of CDP has been investigated by Ebbert [7]. Jenkin [8] and Artmann *et al.* [9] have written on the calculation of CDP and interpretation of results. Finally, Jenkin has written on fast estimation of CDP [10]. Two uniform tone patches, representing the brightest and darkest components of a desired contrast level, are recorded in chosen illumination conditions by the imaging system under analysis. The patches should be large enough that a reasonable statistical sampling of the noise processes of the imaging system are captured. Typically, 10×10 pixels in the final image for each is sufficient. After transformation of the patch data into linear input units via the system tone curve, calculation proceeds by evaluating the contrast of every pixel combination between the two patches to estimate a distribution of contrasts, Figure 1. CDP for the contrast, illumination and system parameters used is then yielded by calculating the proportion of the distribution within the given limits. This procedure may then be repeated to calculate CDP values for different illumination and contrast combinations.

Bounds for the calculation are chosen based on the contrast type used and the application for which the CDP calculation is intended. As noise increases, the probability that two pixels will yield a contrast level within the desired bounds decreases and conversely, as noise improves, so the probability of correctly recording the contrast also rises. Geese *et al.* suggest that the output from CDP may be correlated to the performance of specific imaging tasks [5] and Jenkin has previously compared CDP to results from detectivity [8].

CDP has a numerical range of zero to one and thus when the distribution of the contrasts is completely within the bounds specified by thresholds used, the value of the metric will saturate at of value of one. The metric indicates that the variation in the contrast is low enough to be sufficient for the task at hand. A disadvantage of this is that, because the metric saturates, any overhead in performance of the imaging system cannot be

evaluated. Figure 2, shows CDP calculated for a simulated 8Mp f1.6 4 exposure HDR camera system with typical parameters for sensitivity and noise. CDP values are plotted against illumination level and target contrast. The system was modelled using approaches previously detailed by Jenkin and Kane [11,12].

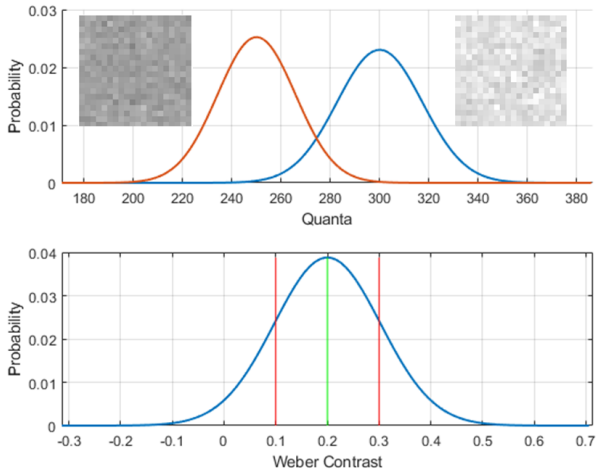

Figure 1, Distribution of Weber contrasts as calculated from recording bright and dark image patches and comparing each combination of pixels.

Weber contrast was used and the threshold for the CDP calculation was set to 10%. It may be seen that the metric saturates for a large proportion of the surface. Values of contrast above 100% are saturated as are values above a luminance of approximately 3 cdm^{-2} as indicated by the horizontal and vertical lines. Contrasts above 100% are common in automotive applications. For example, a traffic sign may easily have a contrast of 500% [5]. The metric is not saturated at the periphery of the area, however, given the number of patch comparisons required to generate the surface, a relatively small number yield values under one. Additionally, any knowledge about the performance of the imaging system, aside from its ability to perform the task at hand, is masked in the areas where the metric is saturated. It should be noted that if there is desire to examine different CDP thresholds, the entire surface has to be recomputed.

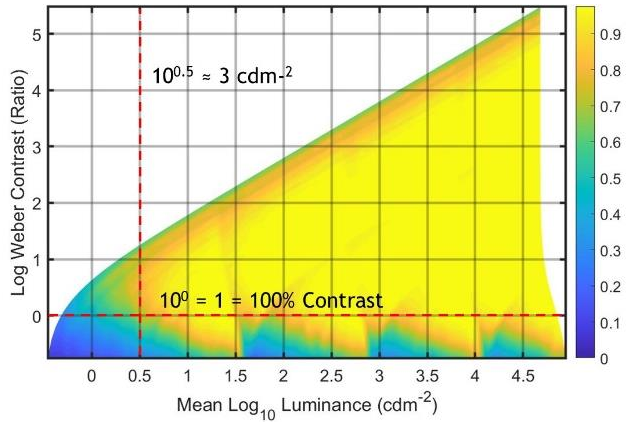

Figure 2, CDP calculated for a simulated 8Mp 2.1µm f1.6 4 exposure HDR system plotted against illumination and target contrast. Weber contrast with bounds of 10% were used for the CDP calculation.

Contrast Signal to Noise Ratio

Contrast to noise ratio has been used previously in medical imaging to determine the performance of imaging systems [3,4] and may be defined as [4]:

$$CNR = \frac{S_A - S_B}{N_{BG}} \tag{3}$$

where S_A is the signal intensity of an area A, S_B the signal intensity of an area B and N_{BG} the background noise. The background noise, N_{BG}, is defined as [4]:

$$N_{BG} = \sqrt{\sigma_A^2 + \sigma_B^2} \tag{4}$$

where σ_A and σ_B are the standard deviations of the noise of each area respectively [4]. The above is similar to a detection theory approach and yields the number of mutual standard deviations separating the two signals [2].

Weber and Michelson contrast both have a highly non-linear mapping with respect to signal separation. Low dark patch values tend to push Weber contrast to a value of infinity quickly and also hold Michelson contrast close to unity regardless of bright patch values. Therefore, it is possible to produce vastly different contrast values with individual patches that have similar signal separations, though shifted slightly in intensity. Therefore, CNR will have a highly non-linear response if used with Weber or Michelson contrast. A way to overcome this issue is to use the standard deviation of the contrast distribution to describe the noise and define therefore contrast signal to noise ratio, CSNR, as below:

$$CSNR = \frac{\bar{C}}{\sigma_C} \tag{5}$$

where $\bar{C}$ is the expected contrast and σ_C the standard deviation of the contrast. Any variation in the contrast is now effectively normalized by the value of the contrast itself.

Figure 3 shows the result of using the above approach to calculate a Weber CSNR surface for the simulation previously described. The metric can be seen not to saturate and changes in CSNR may be seen at transition regions between the individual exposures comprising the combined HDR image from the system. Point A in Figure 3 shows a region where slight changes in the contrast or illumination of a target may cause large changes in CSNR. This would indicate an area in the operational space of the sensor that engineers may wish to examine more closely to ensure overall system performance.

Because CSNR does not saturate, it is possible to also assess performance overhead in the system providing an idea of the safety margin available for a given contrast and illumination condition. If, however, the area of the surface that meets a required imaging condition is required in a similar manner to CDP, it is possible to achieve this by thresholding the CSNR surface, Figure 4. It may be seen that the CSNR surface with the threshold applied is a very similar shape to that directly calculated using CDP. Applying further thresholds to explore alternative tolerances is trivial and does not require recomputing the patch combinations.

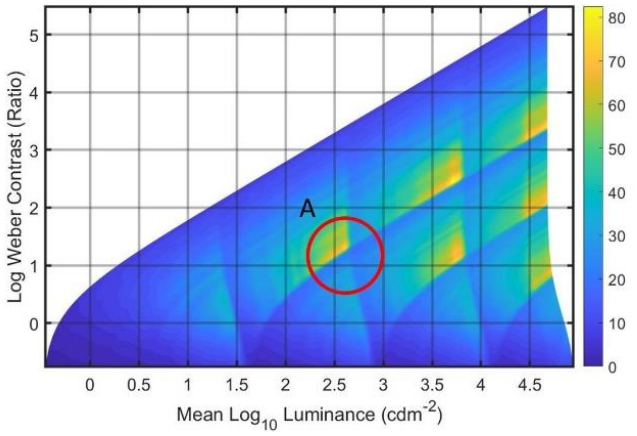

Figure 3, A Weber CSNR surface calculated for the simulated 8Mp system. Point A shows a region where image quality changes quickly due to transition regions in the HDR exposure scheme.

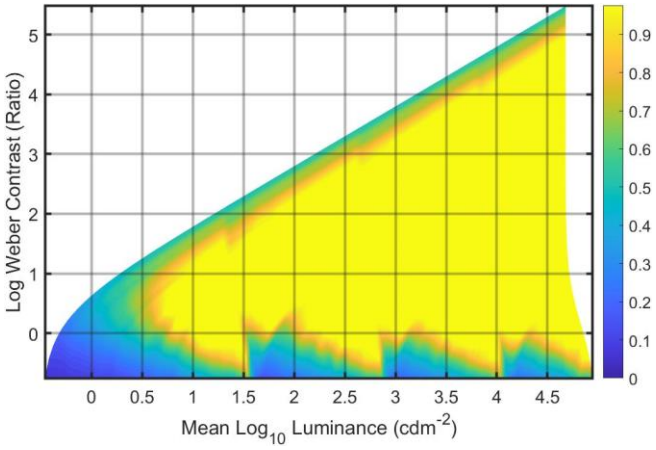

Figure 4, A proxy CDP surface generated by thresholding the CSNR surface at a ratio of 18. The area of acceptable performance is very similar to that outlined by the direct CDP calculation.

Detectivity

Detection theory is used to describe the ability of a system to statistically separate given signals [2]. In the case of an imaging system this would be to distinguish a target from a background and it is generally expressed in terms of mutual standard deviations of noise separation between expected signals from a test to detect the target or the background. This is the SNR of the test process. For an idealized observer, SNR_I may be written [2]:

$$SNR_I = \sqrt{\frac{(t_2-t_1)^2}{1/2(\delta_1^2+\delta_2^2)}} \tag{6}$$

where $\langle t \rangle_n$ is the expected value of the test and σ_n the standard deviation associated with each hypothesis. A summary of the idealized observer result derived from statistical decision theory is given by Kane [1]. Other treatments of the topic may be found in [2,13,14].

It is possible to show that CSNR is proportional to SNR_I for a cobblestone target for a given area and contrast. The mean of the contrast, $\bar{C}$, is estimated as:

$$\bar{C} = \frac{E_{MAX}}{E_{MIN}} - 1 \tag{7}$$

where E_{MAX} and E_{MIN} are the maximum and minimum patch signals respectively expressed in quanta. The mean signal, $\bar{L}$, expressed in quanta is:

$$\bar{L} = \frac{E_{MAX}+E_{MIN}}{2} \tag{8}$$

Rewriting E_{MAX} and E_{MIN} in terms of $\bar{L}$ and $\bar{C}$ using equations (7) and (8):

$$E_{MIN} = \frac{2\bar{L}}{\bar{C}+2} \tag{9}$$

$$E_{MAX} = \frac{2\bar{L}\bar{C}+2\bar{L}}{\bar{C}+2} \tag{10}$$

Considering a cobblestone of area A with shot noise, the signal and standard deviations of dark and bright patches, t_1, t_2, σ_1 and σ_2 are:

$$t_1 = E_{MIN}.A \tag{11}$$

$$t_2 = E_{MAX}.A \tag{12}$$

$$\sigma_1 = \sqrt{E_{MIN}}.\sqrt{A} \tag{13}$$

$$\sigma_2 = \sqrt{E_{MAX}}.\sqrt{A} \tag{14}$$

Substituting these into equation (6), the SNR_I for a cobblestone target ignoring MTF is:

$$SNR_I = \sqrt{\frac{(A.E_{MAX}-A.E_{MIN})^2}{0.5(E_{MAX}.A+E_{MIN}.A)}} \tag{15}$$

Substituting (9) and (10) into (15) and simplifying we may rewrite SNR_I in terms of L and C:

$$SNR_I = \sqrt{\frac{4\bar{C}^2\bar{L}A}{(\bar{C}+2)^2}} \tag{16}$$

Rearranging (16) to give $\bar{L}$ we find:

$$\bar{L} = \frac{SNRI^2(\bar{C}+2)^2}{4\bar{C}^2A} \tag{17}$$

Via Griffin [15], the variance of Weber Contrast, if considering shot noise, V_C, may be estimated as [10]:

$$V_c = \frac{E_{MAX}}{{E_{MIN}}^2} + \frac{{E_{MAX}}^2}{{E_{MIN}}^3} \tag{18}$$

Additionally:

$$V_c = \sigma_C^2 \tag{19}$$

Using equations (5), (7), (18) and (19), the Contrast SNR, CSNR, may be written:

$$CSNR = \frac{\bar{C}}{\sqrt{V_c}} = \frac{\frac{E_{MAX}}{E_{MIN}} - 1}{\sqrt{\frac{E_{MAX}}{{E_{MIN}}^2} + \frac{{E_{MAX}}^2}{{E_{MIN}}^3}}} \quad (20)$$

Substituting (9) and (10) into (20) and simplifying we may also rewrite CSNR in terms of $\bar{L}$ and $\bar{C}$:

$$CSNR = \frac{\sqrt{2}\bar{C}}{\sqrt{\frac{(\bar{C}+1)(\bar{C}+2)^2}{\bar{L}}}} \quad (21)$$

Rearranging (21) to give $\bar{L}$ we find:

$$\bar{L} = \frac{CSNR^2(\bar{C}+1)(\bar{C}+2)^2}{2\bar{C}^2} \quad (22)$$

Equations (17) and (22) write $\bar{L}$ in terms of SNR_I, CSNR, A and $\bar{C}$. By being able to do this we show that SNR_I and CSNR are linked only by contrast and area for any given luminance. Setting equation (17) equal to (22):

$$\frac{CSNR^2(\bar{C}+1)(\bar{C}+2)^2}{2\bar{C}^2} = \frac{{SNR_I}^2(\bar{C}+2)^2}{4\bar{C}^2 A} \quad (23)$$

Multiplying (23) by $4\bar{C}^2A$, and dividing by $CSNR^2(\bar{C}+2)^2$ yields:

$$2(\bar{C}+1)A = \frac{{SNR_I}^2}{CSNR^2} \quad (24)$$

Taking roots and multiplying by CSNR we find:

$$SNR_I = \sqrt{2(\bar{C}+1)A}.CSNR \quad (25)$$

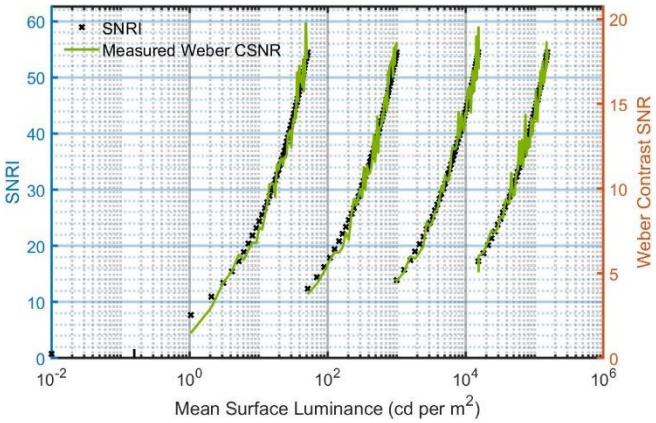

Figure 5, Weber CSNR calculated for a 10x10cm 90% reflective object against a 10% reflective background for the 8Mp 2.1μm system compared against SNR_I for the same. The CSNR has been scaled using equation (25) to demonstrate the proportionality.

Therefore, for a cobblestone target, area A, and contrast $\bar{C}$, SNR_I is proportional to CSNR via equation (25) at all luminance levels. Figure 5 shows a plot of CSNR calculated for a 10x10cm object with 90% reflectance against a 10% reflective background imaged using the simulated 8Mp f1.6 system as described previously. It can be seen there is good alignment between the SNR_I calculated for the system versus that derived from the measured and scaled CSNR.

One useful aspect of calculating SNR_I is that, once mutual standard deviations of separation between a target and background have been established, a standard normal distribution table may be used to calculate true and false positive rates to yield the detection error rates likely to be achieved by the system.

Summary

Contrast signal to noise ratio (CSNR) was introduced and compared to contrast detection probability (CDP). It was shown that CSNR may be calculated without pre-determined thresholds and does not saturate. This in turn enables performance overhead to be evaluated and information to be generated in regions of interest of the operational envelope of the imaging system where CDP reaches its maximum value. A CDP type surface was shown to be generated by applying a threshold to the CSNR result. CSNR was further mathematically linked to the idealized observer for a cobblestone target enabling the estimation of detection error rates.

References

[1] P. Kane, ‘‘Signal detection theory and automotive imaging,’’ IS&T Electronic Imaging: Autonomous Vehicles and Machines 2019 Proceedings (IS&T, Springfield, VA, 2019), pp. 027-1–027-7(7).

[2] ICRU Report 54, Medical Imaging – The Assessment of Image Quality, Bethesda MD: International Commission on Radiation Units and Measurements, 1996.

[3] F. Timischl, ‘‘The Contrast-to-Noise Ratio for Image Quality evaluation in Scanning Electron Microscopy,’’ Scanning, Vol. 37, 54-62 (2015).

[4] Desai, Nikunj & Singh, Abhinav & Valentino, Daniel. (2010). Practical Evaluation of Image Quality in Computed Radiographic (CR) Imaging Systems. Proceedings of SPIE - The International Society for Optical Engineering. 7622. 10.1117/12.844640.

[5] M. Geese, U. Seger, and A. Paolillo, ‘‘Detection probabilities: performance prediction for sensors of autonomous vehicles,’’ IS&T Electronic Imaging: Autonomous Vehicle and Machines 2018 Proceedings (IS&T, Springfield, VA, 2018), pp. 148-1–148-14(14).

[6] IEEE Autonomous Imaging White Paper, The Institute of Electrical and Electronics Engineers, Inc., 3 Park Avenue, New York, NY 10016-5997

[7] L. Ebbert, “Implementation of CDP”, Bachelor Thesis, University of Applied Sciences Dusseldorf, 2018.

[8] Jenkin, R. B., “Comparison of Detectability Index and CDP” Journal of Imaging Science and Technology, Volume 63, Number 6, November 2019, pp. 60405-1-60405-9(9)

[9] Artmann, U., et al., “Contrast detection probability - Implementation and use cases”, Electronic Imaging, Autonomous Vehicles and Machines Conference 2019, pp. 30-1-30-13(13), Society for Imaging Science and Technology, DOI: https://doi.org/10.2352/ISSN.2470-1173.2019.15.AVM-030

[10] Jenkin, R., B., Fast Prediction of Contrast Detection Probability, Proc. IS&T Electronic Imaging, Autonomous Vehicles and Machines 2020, Burlingame, California, 2020.

[11] R. Jenkin and P. Kane, “Fundamental Imaging System Analysis for Autonomous Vehicles”, Proc. IS&T Electronic Imaging, Autonomous Vehicles and Machines 2018, Burlingame, California, 2018.

[12] Jenkin, R., B., Radiometry and Photometry for Autonomous Vehicles and Machines - Fundamental Performance Limits, Proc. IS&T Electronic Imaging, Autonomous Vehicles and Machines 2021, Burlingame, California, 2021.

[13] H. H. Barrett, K. Myers, Foundations of Image Science, Wiley, 2004.

[14] J. Beutel, H. Kundel, Van Metter R., Handbook of Medical Imaging Vol. 1, SPIE Press 2000

[15] Griffin, T. F., “A thesis in statistics”, Texas Tech University, 1992.

Author Biography

Robin Jenkin received, BSc(Hons) Photographic and Electronic Imaging Science (1995) and his PhD (2001) in the field of image science from University of Westminster. He also holds a M.Res Computer Vision and Image Processing from University College London (1996). Robin is a Fellow of The Royal Photographic Society, UK, and a board member and VP Publications of IS&T. Robin works at NVIDIA Corporation where he models image quality for autonomous vehicle applications. He is a Visiting Professor at University of Westminster within the Computer Vision and Imaging Technology Research Group.

JOIN US AT THE NEXT EI!

IS&T International Symposium on

Electronic Imaging

SCIENCE AND TECHNOLOGY

Imaging across applications . . . Where industry and academia meet!

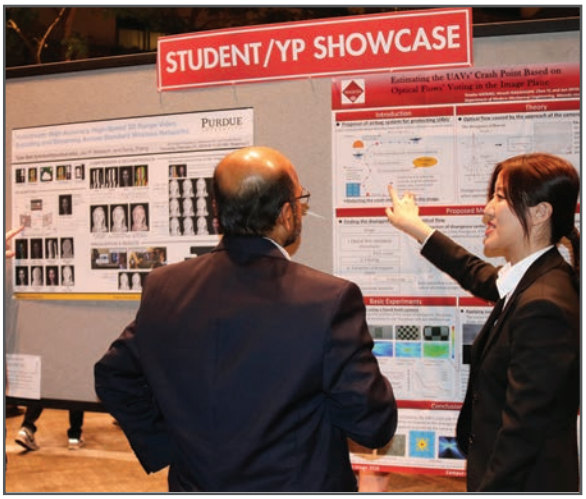

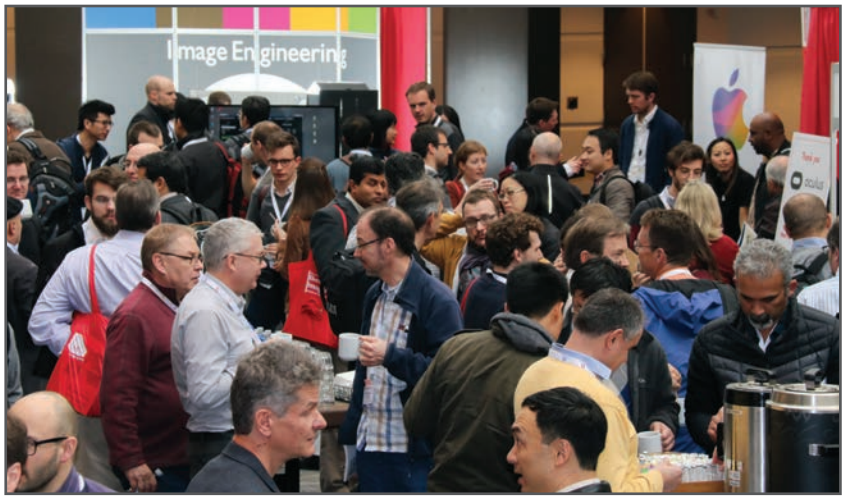

• SHORT COURSES • EXHIBITS • DEMONSTRATION SESSION • PLENARY TALKS •
• INTERACTIVE PAPER SESSION • SPECIAL EVENTS • TECHNICAL SESSIONS •

www.electronicimaging.org

IS&T
imaging.org